The Journal of Chemical Physics ARTICLE scitation.org/journal/jcp

Two-step nucleation in a binary mixture of patchy particles

Cite as: J. Chem. Phys. 158, 154502 (2023); doi: 10.1063/5.0140847
Submitted: 31 December 2022 • Accepted: 24 March 2023 •
Published Online: 17 April 2023

Camilla Beneduce,[1] Diogo E. P. Pinto,[1] Petr Šulc,[2,3] Francesco Sciortino,[1] and John Russo[1,a)]

AFFILIATIONS

[1] Dipartimento di Fisica, Sapienza Università di Roma, Piazzale Aldo Moro 5, 00185 Rome, Italy
[2] School of Molecular Sciences and Center for Molecular Design and Biomimetics, The Biodesign Institute, Arizona State University, 1001 South McAllister Avenue, Tempe, Arizona 85281, USA
[3] Life and Medical Sciences (LIMES), University of Bonn, 53121 Bonn, Germany

Note: This paper is part of the JCP Special Topic on Nucleation: Current Understanding Approaching 150 Years After Gibbs.
[a)] **Author to whom correspondence should be addressed:** john.russo@uniroma1.it

ABSTRACT

Nucleation in systems with a metastable liquid–gas critical point is the prototypical example of a two-step nucleation process in which the appearance of the critical nucleus is preceded by the formation of a liquid-like density fluctuation. So far, the majority of studies on colloidal and protein crystallization have focused on one-component systems, and we are lacking a clear description of two-step nucleation processes in multicomponent systems, where critical fluctuations involve coupled density and concentration inhomogeneities. Here, we examine the nucleation process of a binary mixture of patchy particles designed to nucleate into a diamond lattice. By combining Gibbs-ensemble simulations and direct nucleation simulations over a wide range of thermodynamic conditions, we are able to pin down the role of the liquid–gas metastable phase diagram on the nucleation process. In particular, we show that the strongest enhancement of crystallization occurs at an azeotropic point with the same stoichiometric composition of the crystal.

INTRODUCTION

The ability to guide dilute solutions of properly designed colloidal particles to spontaneously turn into specific ordered structures is crucial for a large-scale application of the self-assembly paradigm.[1,2] One relevant example of this strategy is provided by the DNA-origami nanotechnology, nowadays a mature methodology, which allows for the design and production of nanometric particles with controllable shape and interactions.[3] It has been demonstrated that these particles, once properly designed, are able to self-assemble into ordered crystalline lattices even starting from quite dilute conditions,[4,5] suggesting the exploitation of complex nucleation pathways that are still not fully understood.

One such pathway is the so-called *two-step nucleation pathway*, in which a metastable gas–liquid transition can spontaneously generate local regions with high particle concentration, thus greatly enhancing the nucleation rate.[6–17] In the last decade, this process has been observed in simple systems that are either one-component systems or ionic compounds: examples include hard particle fluids,[18] colloids,[11,19,20] salt solutions,[21] and calcium carbonate.[22,23] Importantly, two-step processes play an important role in the crystallization of globular proteins.[19,24–27] For colloidal particles, globular proteins, and non-globular proteins, the short-range nature of the inter-particle interaction generates a metastable gas–liquid coexistence, which provides a mechanism for locally enhancing the density and triggering crystal formation. Spinodal decomposition and/or liquid-phase nucleation are equally active mechanisms. In addition, ten Wolde and Frenkel[19] have called attention to the possibility to exploit critical fluctuations as a mechanism for locally increasing density. In all these cases, a two-step nucleation process takes place, the first step being the local increase of density and the second being the formation of a crystal nucleus in one or several of such enhanced density regions.

The crystallization of specific crystal structures is not devoid of problems.[28,29] Kinetic pathways can drive the assembly toward amorphous aggregates or crystals different from the desired one. To address this last case, several strategies have been suggested; examples include optimization of preparation protocols,[30–32] the

accurate design of the interparticle potential,[29,33–40] or geometrical approaches where inter-particle interactions are made to match the geometric features of the target structure.[41–48] Rather than increasing the complexity of inter-particle interactions, another successful strategy is to increase the number of building blocks. When the building blocks are modeled as patchy colloids, i.e., particles with specific directional interactions, the process of designing the bonding rules to assemble one specific crystal (and selectively avoid the formation of any other competing structure) can be turned into a set of Boolean satisfiability (SAT) equations, which can be solved using modern SAT solver algorithms. This strategy, named *SAT-assembly*, was shown to lead to the successful assembly of several complex target structures, including the coveted colloidal diamond crystal.[49–51]

Compared to the one-component case, crystal formation and two-step pathways in multi-component systems have received much less attention. In these systems, composition fluctuations couple with density fluctuations and it is not *a priori* clear if the stoichiometric properties of the spontaneously generated liquid phase are consistent with the corresponding properties of the selected crystal. Even when the components are fully miscible in the solid phase (such as Pd and Ag), it was shown that the competition between demixing and crystallization has a big impact on the growth process, causing large variations in the radial composition of the nuclei.[52] Multi-component systems also display thermodynamic behavior that is not found in one-component systems, such as lines of binary critical points, azeotropic points, and re-entrant condensation. Experimental studies have already shown that phase separation in multi-component systems does not preserve the original ratio between the different species and that the phase behavior strongly depends on the components ratio,[53–55] but it is yet unclear whether some of the peculiar multi-component mixture features can affect crystal nucleation.

In this article, we use extensive computer simulations of a binary mixture of patchy particles that self-assembles in a diamond crystal with a fixed stoichiometric ratio, with the goal of relating the phase behavior of the mixture to its crystallization pathway. This article is organized as follows. In the section titled Methods, we introduce the N2c8 binary mixture and briefly summarize its phase behavior. Numerically, we obtain the phase diagram with Gibbs ensemble simulations, while the crystallization behavior is observed via direct Monte Carlo simulations. We make use of biased moves to accelerate diffusional times and observe crystallization for state points where the free-energy barrier can be overcome by thermal fluctuations during our simulation times. The section titled Results will superimpose the metastable phase diagram with histograms of the nucleation rate, confirming the two-step nucleation pathway and allowing us to study the relation between demixing and crystallization. In the section titled Discussion and Conclusions, we put our results in the wider context of empty liquids and argue that while the two-step nucleation pathway is an effective strategy to overcome diffusional barriers, azeotropic points are the key to lower compositional barriers.

METHODS

We choose patchy particles as our model system: they describe systems with hard-core isotropic repulsion and attractive directional interactions. Experimentally, anisotropic interactions can be obtained either via the shape[56] or via chemical patterning of the surface,[57–61] for example, by attaching single strands of DNA to well-defined positions on their surface.[61–66] We represent them computationally via the Kern–Frenkel[67,68] potential, in which hard-core spherical particles of diameter σ interact with a square well potential V_{SW} of depth ϵ and width δ, modulated by a term f depending on the relative orientation of the particles: in particular, two patchy particles can establish a *bond* if their centers are at distance between σ and $\sigma+\delta$ and if the line connecting their centers intersects the volume of both patches involved in the bond. In the following, we measure energy in units of the square-well depth (ϵ) and distances in units of the patchy particle diameter (σ). Mathematically, the interaction between particles i and j is described by

$$V(\mathbf{r}_{ij},\hat{\mathbf{r}}_{\alpha,i},\hat{\mathbf{r}}_{\beta,j}) = V_{SW}(r_{ij}) f(\mathbf{r}_{ij},\hat{\mathbf{r}}_{\alpha,i},\hat{\mathbf{r}}_{\beta,j}), \tag{1}$$

where $\hat{\mathbf{r}}_{\alpha,i}$ ($\hat{\mathbf{r}}_{\beta,j}$) indicates the position of patch α (β) of particle i (j) and

$$f(\mathbf{r}_{ij},\hat{\mathbf{r}}_{\alpha,i},\hat{\mathbf{r}}_{\beta,j}) = \begin{cases} \Upsilon_{(\alpha,i)\,(\beta,j)} & \text{if } \hat{\mathbf{r}}_{ij}\cdot\hat{\mathbf{r}}_{\alpha,i} > \cos(\theta_{max}), \\ & \hat{\mathbf{r}}_{ji}\cdot\hat{\mathbf{r}}_{\beta,j} > \cos(\theta_{max}), \\ 0 & \text{otherwise.} \end{cases} \tag{2}$$

$\Upsilon_{(\alpha,i)(\beta,j)}$ is the (color) interaction matrix element and is equal to 1 if patch α on particle i interacts with patch β on particle j and 0 otherwise. $\boldsymbol{\Upsilon}$ is a matrix that encodes the interactions between both identical and distinct species. Finding the interaction matrix that will guide the system to self-assemble into a desired structure can be cast into an *inverse self-assembly* problem, whose solution can be found with the *SAT-assembly* algorithm.[49,50]

We run two types of simulations: Gibbs-ensemble simulations to determine the liquid–gas coexistence line and NVT Monte Carlo simulations in an extensive range of densities (ρ) and relative concentrations (x, i.e., the fraction of species 2).

We fix the parameters of the Kern–Frenkel potential to $\cos(\theta_{max}) = 0.98$ and $\delta = 0.2$, for which nucleation is readily accessible within simulation times. Moreover, direct simulations take advantage of aggregation-volume-bias (AVB) moves[69] to accelerate the dynamics of bond-formation and bond-breaking. Both methods have been described in more detail in Ref. 70. We confirmed with independent simulations that nucleation events are also observed in unbiased simulations, albeit requiring longer simulation times.

Our goal is to study the nucleation process in multi-component mixtures, such as the binary mixture described by the N2c8 interaction matrix (so called because it has two species and eight colored patches), which was originally introduced as a SAT-assembly solution to the problem of assembling the cubic diamond crystal, while avoiding the hexagonal diamond crystal.[51] The ability to suppress a competing polytype, thus avoiding the formation of stacking faults, makes this mixture a candidate for the experimental realization of photonic crystals. The N2c8 solution is graphically depicted in Fig. 1: two patchy particle species differing in patch types (colors); patches with matchable colors that can bind with each other are reported in the bottom part of the table. This mixture crystallizes in the diamond-cubic phase and notably cannot form the hexagonal diamond.

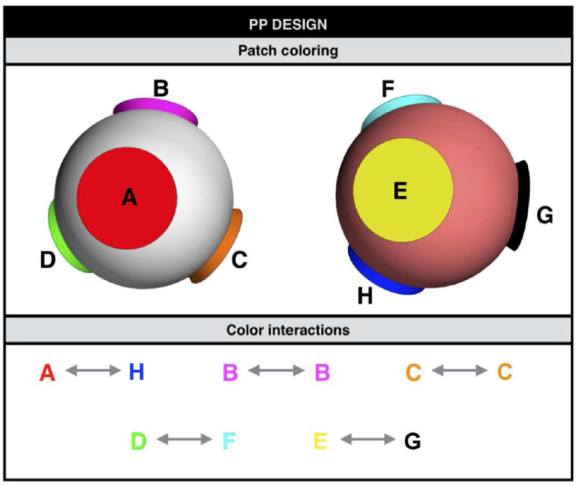

FIG. 1. 3D representation of the azeotropic N2c8 solution SAT-designed to self-assemble a cubic diamond crystal lattice. It consists of two patchy particles species (N2), the gray and the red one differing in the patch types. The patch types/different colors are eight (c8) referred to by letters A through H. Patches that can bind with each other are reported in the bottom part of the table.

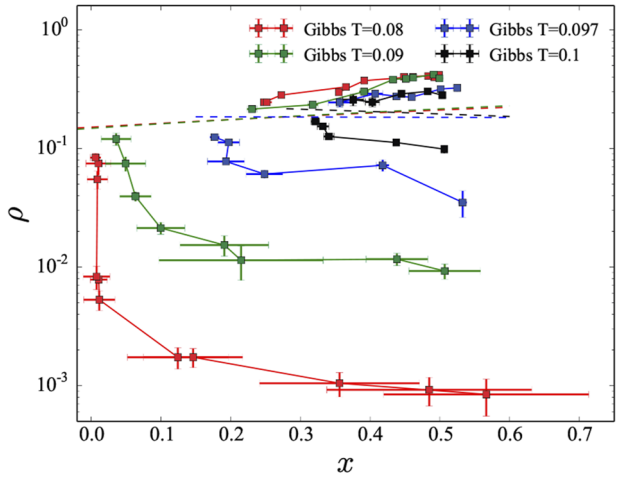

FIG. 3. SAT-designed N2c8 binary mixture density-concentration phase diagrams for different temperatures T expressed in unit of k_B/ϵ; the coexistence region shrinks by increasing the temperature. Each binodal curve is obtained by Monte Carlo simulations with AVB moves in the Gibbs ensemble.[69] In particular, for temperatures $T = 0.08$ and $T = 0.09$, 500 particles were simulated, while for temperatures $T = 0.097$ and $T = 0.1$, 1000 particles were considered. Dashed lines are rectilinear diameter lines indicating where critical points are located. The lines for $T = 0.08$ and $T = 0.09$ are almost superimposed.

We highlight that the results presented in the section titled Results for the N2c8 solution are general; we focus on this binary mixture since it is a meaningful example and since we already know its phase behavior. Indeed, the phase diagram of the mixture was studied within Wertheim thermodynamic perturbation theory in Ref. 70, whose results we summarize in Fig. 2. The N2c8 mixture has a reentrant binary critical point line, which goes to zero temperature and pressure as the pure components are approached. This behavior is immediately apparent from the color design of Fig. 1, where it can be seen than each species can form only two intra-species bonds, so when the system is made of only one component, it can only form linear chains and thus does not have a critical point at any finite temperature.[71] The non-ideal nature of the mixture manifests itself in a line of azeotropic points at $x = 1/2$. Along such a line, the system

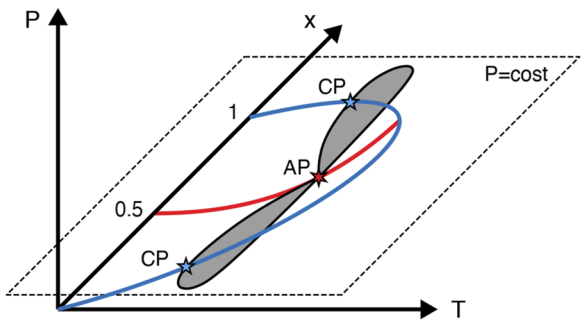

FIG. 2. Schematic PTx phase diagram of the N2c8 solution. The blue line is the binary critical point line, which goes to $(P, T) \to 0$ for $x \to (0, 1)$. The red line, in the plane $x = 0.5$, represents the line of azeotropic points. The shaded area represents the coexistence region on a isobaric surface.

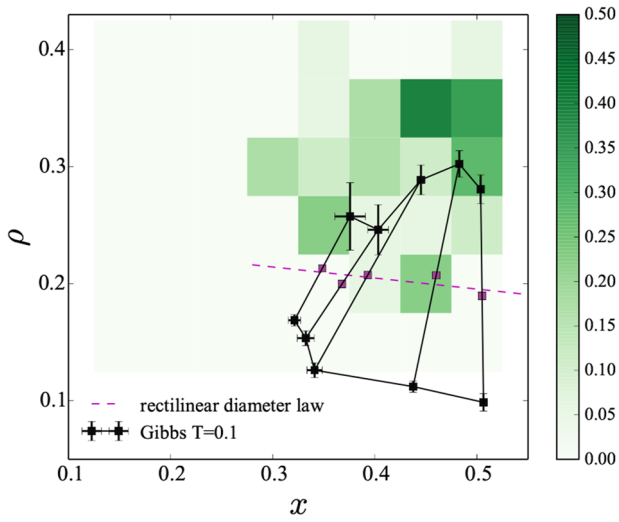

FIG. 4. Nucleation plot for temperature $T = 0.1$ (in unit of k_B/ϵ). The binodal black curve obtained via Monte Carlo simulations in the Gibbs ensemble is superimposed to a green colormap reporting, for each considered state point, the ratio between the number of trajectories that nucleate over the total number of trajectories analyzed. We considered as successfully assembled the runs exhibiting a fraction of particles in the cubic diamond phase greater or equal to 0.2. Examined state points belong to the regular grid with $\rho \in [0.15, 0.4]$ and $x \in [0.15, 0.5]$, where $\Delta\rho = 0.05$ and $\Delta x = 0.05$. For each state point (centered in each rectangular of the colormap), several Monte Carlo simulations were run with 500 particles and AVB dynamics in the NVT ensemble. In particular, we made ten runs for each state point whose $x \leq 0.25$ and we increased them to 18 for state points with $x \geq 0.3$. Purple squares represent averages of each pair of coexisting points, and according to the rectilinear diameter law, the best straight line passing through them (the dashed line) provides an indication of where the critical point is.

always demixes at the same composition, i.e., the liquid phase will have an equimolar composition of both species. As we will see, this is particularly relevant for the nucleation process as the crystal also has an equimolar composition. In the section titled Results, we will look at the interplay between phase separation and nucleation.

To identify crystal particles, we use local bond-order analysis.[72] A $(2l+1)$-dimensional complex vector $(\mathbf{q}_l)$ is defined for each particle i as $q_{lm}(i) = \frac{1}{N_b(i)} \sum_{j=1}^{N_b(i)} Y_{lm}(\hat{\mathbf{r}}_{\mathbf{ij}})$, where we set $l = 12$ and m is an integer that runs from $m = -l$ to $m = l$. The functions Y_{lm} are the spherical harmonics, and $\hat{\mathbf{r}}_{\mathbf{ij}}$ is the normalized vector from particle i to particle j. The sum goes over the first $N_b(i) = 16$ neighbors of particle i. We then introduce a spatial coarse-graining step $Q_{lm}(i) = \frac{1}{N_b(i)} \sum_{k=0}^{N_b(i)} q_{lm}(k)$.[73] The scalar product between $Q_{12,m}$ of

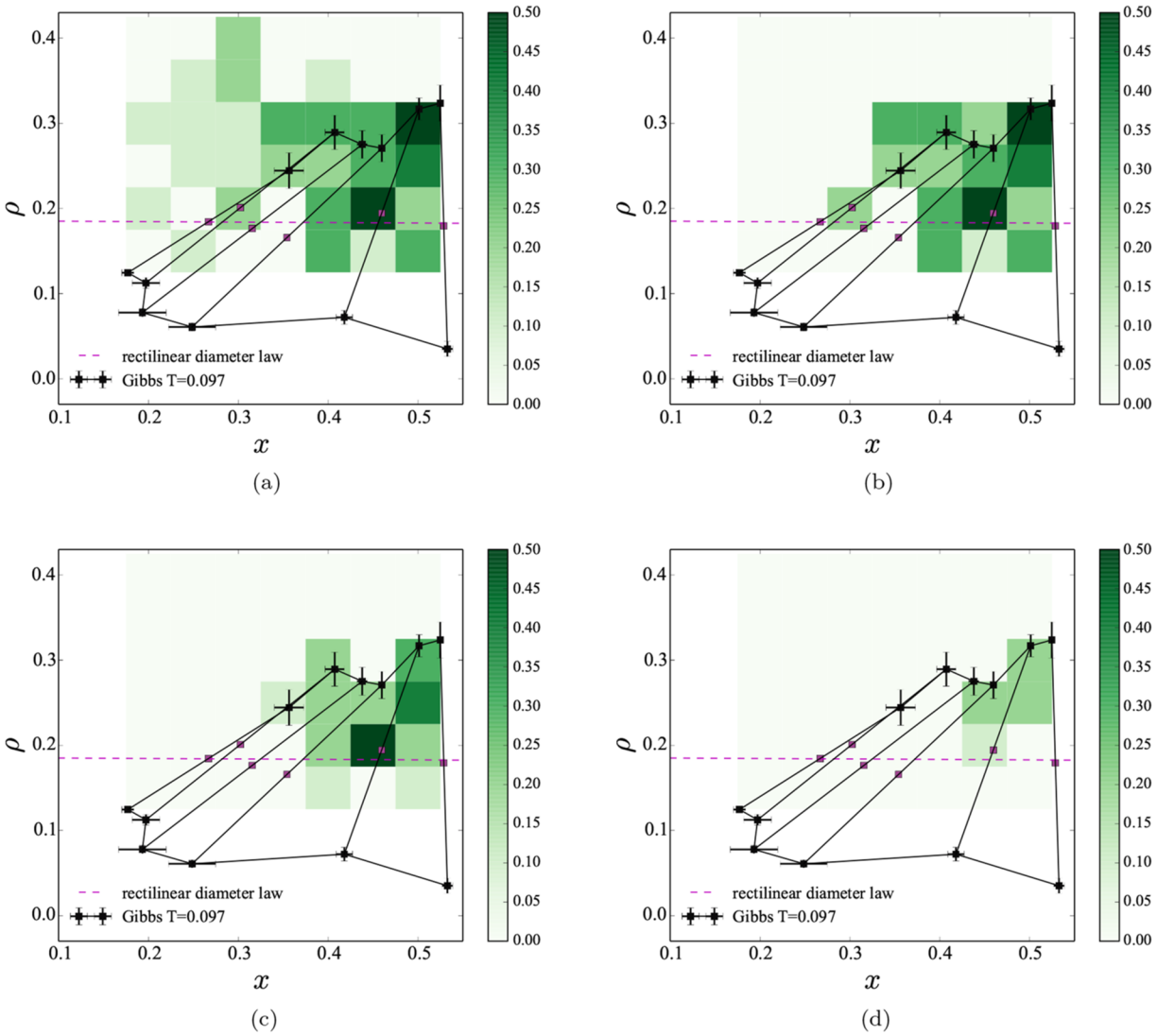

FIG. 5. Nucleation plots for temperature $T = 0.097$ (in unit of k_B/ϵ). The binodal black curve obtained via Monte Carlo simulations in the Gibbs ensemble is superimposed to a green colormap reporting, for each considered state point, the ratio between the number of trajectories that nucleate over the total number of trajectories analyzed. We considered as successfully assembled the runs exhibiting a fraction of particles in the cubic diamond phase (t) greater or equal to 0.2 in (a), 0.5 in (b), 0.7 in (c), and 0.9 in (d). Examined state points belong to the regular grid with $\rho \in [0.15, 0.4]$ and $x \in [0.2, 0.5]$, where $\Delta\rho = 0.05$ and $\Delta x = 0.05$. For each state point (centered in each rectangular of the colormap) were run ten Monte Carlo simulations with 1000 particles and AVB dynamics in the NVT ensemble. Purple squares represent averages of each pair of coexisting points, and according to the rectilinear diameter law, the best straight line passing through them (the dashed line) provides an indication of where the critical point is. Nucleation occurs for almost each considered state point, but the extended cubic diamond lattice $(t \geq 0.7)$ can appear only close to the liquid branch and to the azeotropic condition.

two particles is defined as $\mathbf{Q}_{12}(i) \cdot \mathbf{Q}_{12}(j) = \sum_m Q_{12,m}(i) Q_{12,m}(j)$. If the scalar product $(\mathbf{Q}_{12}(i)/|\mathbf{Q}_{12}(i)|) \cdot (\mathbf{Q}_{12}(j)/|\mathbf{Q}_{12}(j)|)$ between two neighbors exceeds 0.75, then the two particles are deemed *connected*. We then identify particle i as crystalline if it is connected with at least 12 neighbors.

RESULTS

We run Gibbs ensemble simulations to determine the coexistence region at different temperatures. These are plotted in Fig. 3 for temperatures $T = 0.08$ (red), $T = 0.09$ (green), $T = 0.097$ (blue), and $T = 0.1$ (black). The binodal line at each temperature is split into a liquid branch, at high densities, and a gas branch, at low densities. The two branches meet at the binary critical point, whose location cannot be estimated with Gibbs ensemble simulations.[74] The phase diagram is plotted only for $x < 0.5$, but it is symmetric with respect to the azeotropic line $x = 0.5$. The critical point is located at the intersection of the binodal line and the rectilinear diameter line (i.e., the line connecting the midpoint of the different tie-lines), which is represented for each temperature as a dashed line in Fig. 3. For temperatures $T = 0.08$ and $T = 0.09$, we run single trajectories, while for temperatures $T = 0.097$ and $T = 0.1$, simulations are averaged over at least eight independent simulations; the statistical noise is due to the difficulty in equilibrating the mixtures at low temperatures.

In Fig. 4, we examine the nucleation behavior by running simulation runs over a grid of state points at $T = 0.1$: $\rho \in [0.15, 0.4]$ with $\Delta\rho = 0.05$ and $x \in [0.15, 0.5]$ with $\Delta x = 0.05$. We run up to 10 (or 18 for state points where nucleation is more probable) independent simulation runs for more than 3×10^8 steps each and measure the fraction of trajectories that have nucleated, which is a quantity proportional to the nucleation rate. In Fig. 4, we define a nucleation event as a run in which at least 20% of the particles are found in a crystalline state, according to the $Q12$ criteria described in the section titled "Methods." In Fig. 4, this fraction is proportional to the color intensity of a tile centered around the state point, and the grid is superimposed on the $T = 0.1$ phase diagram. Figure 4 shows that nucleation occurs in correspondence to the liquid–gas coexistence region, with the probability of nucleation being approximately the highest along the liquid binodal. We note, in fact, that no nucleation events are observed at low concentrations, from $x = 0.15$ to $x = 0.25$, i.e., outside the phase coexistence region. Visual inspection of the nucleation trajectories confirms that the nucleation event is preceded by the formation of a dense liquid phase mostly via spinodal decomposition (i.e., liquid drops do not nucleate, but instead, a coarsening liquid network appears at the start of simulations).

To confirm the results of Fig. 4, we run nucleation trajectories in a density-concentration grid at a lower temperature, $T = 0.097$, which makes the coexistence region wider. The results are represented in Fig. 5(a). Compared to the case at $T = 0.1$, now, nucleation events occur over a much wider region of the phase diagram, following the widening of the coexistence region.

These results confirm the observations that were made for one-component systems, i.e., that density fluctuations promote nucleation.[11,15,19,75] However, compared to one-component systems, in a multi-component system, there are both density and concentration fluctuations. Since the crystal has a fixed stoichiometric composition, the formation of a liquid phase at concentrations different from equimolarity is expected to slow down and limit the growth of the crystal. We show this effect in the four panels of Fig. 5, where the colored grid plots the fraction of independent trajectories whose crystalline particles include at least 20% (a), 50% (b), 70% (c), and 90% (d) of the whole system. Figure 5 shows that, while small crystals can form along coexistence regions, the formation of larger crystals is progressively shifted toward the $x = 0.5$ line, i.e., toward the azeotropic point. At the azeotropic point, in fact, the liquid phase forms with the same stoichiometric composition of the crystal.

As demonstrated originally in Ref. 19, critical fluctuations are able to trigger crystal nucleation. We find here that in a binary mixture, it is the azeotropic point that more strongly promotes crystallization. The azeotropic point and the critical point coincide where the two corresponding thermodynamic lines meet (see Fig. 2), which corresponds to the maximum critical temperature at $x = 0.5$. In Fig. 6, we study the nucleation behavior in the density–temperature plane at $x = 0.5$. The nucleation of the diamond cubic occurs again in correspondence to the phase separation, confirming that nucleation is aided by the formation of dense liquid regions during the phase-separation process. We observe that nucleation not only occurs in correspondence to the critical point, but, interestingly, we observe nucleation events at supercritical conditions. The system thus shows two-step nucleation aided both by spinodal decomposition at sub-critical temperatures and by critical fluctuations at super-critical conditions, just as predicted in Ref. 19. While the prediction was made for isotropic one-component systems (globular proteins), at the azeotropic conditions of Fig. 6, the

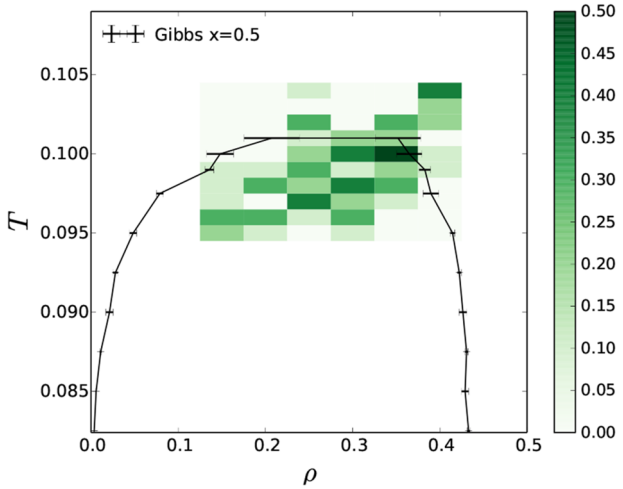

FIG. 6. Equimolar nucleation plot showing that nucleation occurs in two steps where there is a previous locally increasing density phenomenon. The binodal black curve obtained via Monte Carlo simulations in the Gibbs ensemble is superimposed to a green colormap reporting, for each considered state point, the ratio between the number of trajectories that nucleate over the total number of trajectories analyzed. We considered as successfully assembled the runs exhibiting a fraction of particles in the cubic diamond phase greater or equal to 0.2. Examined state points belong to the regular grid with $\rho \in [0.15, 0.4]$ and $T \in [0.095, 0.105]$, where $\Delta\rho = 0.05$ and $\Delta T = 0.001$. For each state point (centered in each rectangular of the colormap), ten Monte Carlo simulations were run with 500 particles and AVB dynamics in the NVT ensemble.

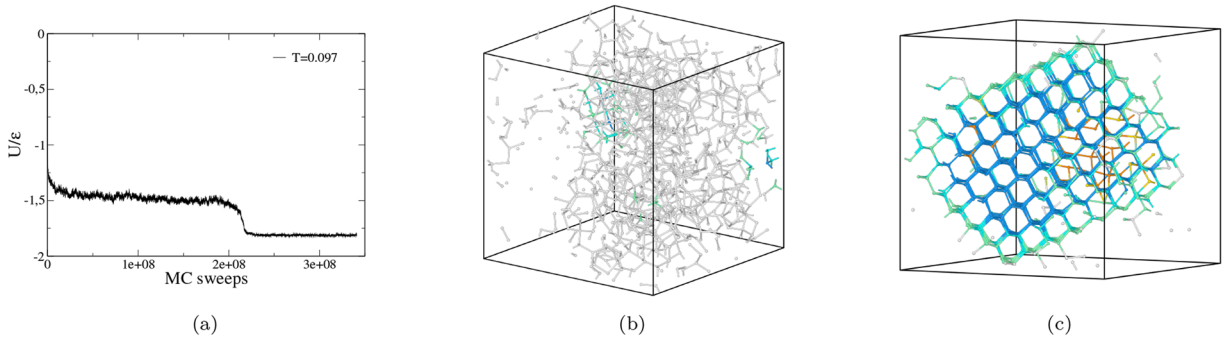

FIG. 7. Overview of Monte Carlo simulation with AVB moves in the NVT ensemble run at $T = 0.097$, $x = 0.5$, and $\rho = 0.3$, where T is in unit of k_B/ϵ and ρ is in unit of $1/\sigma^3$. (a) Potential energy per particle as a function of MC sweeps: the energy drop signals a nucleation event. (b) Snapshot of a metastable configuration before the energy drop, showing that we deal with a two-step nucleation since crystalline nucleus arises in the denser liquid phase. (c) Snapshot of the last configuration, showing that the N2c8 binary mixture eventually self-assembles into a cubic diamond crystal. Neither patches nor the two patchy particles species are shown while blue/green colors indicate particles belonging to the cubic diamond phase. Snapshots and crystal identification are obtained with the Ovito software.[76]

system is indeed thermodynamically equivalent to a one component system.[70]

In Fig. 7, we show the evolution of a typical nucleation trajectory at the azeotropic point at $T = 0.097$ and $\rho = 0.3$. Figure 7(a) shows the evolution of the energy, displaying a two-step drop: initially, the system is prepared in a metastable gas phase, which then forms a percolating liquid phase; in the second step (from 1.9×10^8 MC sweeps), the nucleation occurs within the liquid drop and a diamond cubic crystal replaces all the liquid phase, finally coexisting with a low-density gas. Figure 7(b) shows a snapshot at the end of the first stage, where a liquid–gas coexistence is established in the box. Figure 7(c) shows a snapshot at the final stage of the trajectory, visually confirming the formation of a large crystal of the diamond cubic phase. The absence of the hexagonal diamond phase and stacking fault defects is a property embedded into the color interactions of the N2c8 mixture, which was designed with this property via the SAT-assembly framework.[51]

DISCUSSION AND CONCLUSIONS

Recent experimental advances hold the promise to fully unlock the potential of systems with directional and specific interactions. In particular, DNA nanotechnology already allows for the fabrication of patchy particles in the form of wireframe DNA origami[4,5,66,77] and gold nanoparticles with selective patterning.[78] DNA strands naturally encode sequence complementary and thus allow for the assembly of structures with the desired interactions: different interacting patches correspond to complementary single DNA strands, and the self-interacting ones correspond to palindromic DNA strands. This class of systems goes under the name of *empty liquids*,[79] which have unique properties compared to simple (hard-sphere-like) systems, such as the existence of low-density stable liquid phases,[80] the ability to crystallize in open crystals,[81] and the potential to model the phase behavior of biological molecules.[82–85]

To obtain a complex target structure (such as a photonic crystal) requires either a complex interaction potential carefully optimized to have the target as free-energy minima or a mixture of simpler building blocks that make the target structure accessible by reducing its overall symmetry (crystal sites are occupied by different species). Recent advances in DNA-nanotechnology, allowing for the design of building blocks with arbitrary interaction rules, are opening the door to this last approach.

Several strategies have been proposed to design the interaction potential in a multi-component system. One such strategy is the SAT-assembly framework, which translates the design problem into a Boolean satisfiability problem.[49,50] The ability to design interaction matrices to self-assemble arbitrary structures is a necessary but not sufficient condition for observing the nucleation of such structures under experimental conditions. These often involve preparing the system in very dilute conditions, from which the classical nucleation rate is severely suppressed by both diffusional and compositional barriers.

Regarding the diffusional barrier, probably the most promising strategy to overcome it is *two-step* nucleation, where the crystal nucleation is aided by the formation of dense liquid drops. This nucleation pathway has been the subject of intense research, especially in the context of one-component systems.

So far, not much work has been devoted to the second barrier, i.e., the compositional barrier, which controls the rate at which a particle of the correct species enters in contact with the incipient nucleus. In this work, we have presented a first study in this direction. We have examined a two-step nucleation process in a binary mixture of patchy particles designed to assemble into cubic diamond. In particular, we have focused on the role of the metastable liquid–gas phase diagram on the nucleation process. Comparing Gibbs ensemble simulations with direct nucleation runs, we have established that nucleating state points coincide with the locus of metastability of the mixture, confirming the relevant role played by thermodynamic instabilities, generating local environments with a density enhanced in comparison to the average value. We have shown that composition effects in multi-component systems play a big role in the growth of the crystal and that crystal growth is enhanced at state points where the emerging liquid phase has a composition close to the stoichiometric composition of the crystal. In the studied system, this corresponds to an azeotropic point at equimolar concentration, $x = 0.5$. We find evidence of critical-like enhanced

nucleation along the binary critical line when this intersects the azeotropic line.

To unlock the promises of nanotechnology to self-assemble new materials with desired mechanical, optical, and thermal properties, a big role will be played by the search of general principles behind the crystallization of multi-component systems. We believe that two-step nucleation, augmented with azeotropic conditions, will be one of such guiding principles.

ACKNOWLEDGMENTS

We acknowledge the CINECA award NNPROT under the ISCRA initiative for the availability of high performance computing resources and support. J.R. and D.E.P.P. acknowledge the support from the European Research Council under Grant No. DLV-759187. This result is part of a project that has received funding from the European Research Council (ERC) under the European Union's Horizon 2020 Research and Innovation Program (Grant Agreement No. 101040035) (to P.Š.).

AUTHOR DECLARATIONS

Conflict of Interest

The authors have no conflicts to disclose.

Author Contributions

C.B. and D.E.P.P. contributed equally to this work.

Camilla Beneduce: Conceptualization (equal); Investigation (equal); Methodology (equal); Supervision (equal); Writing – original draft (equal); Writing – review & editing (equal). **Diogo E. P. Pinto**: Conceptualization (equal); Investigation (equal); Methodology (equal); Supervision (equal); Writing – original draft (equal); Writing – review & editing (equal). **Petr Šulc**: Conceptualization (equal); Investigation (equal); Methodology (equal); Writing – original draft (equal); Writing – review & editing (equal). **Francesco Sciortino**: Conceptualization (equal); Investigation (equal); Methodology (equal); Supervision (equal); Writing – original draft (equal); Writing – review & editing (equal). **John Russo**: Conceptualization (equal); Investigation (equal); Methodology (equal); Supervision (equal); Writing – original draft (equal); Writing – review & editing (equal).

DATA AVAILABILITY

The data that support the findings of this study are available from the corresponding author upon reasonable request.

REFERENCES

[1]S. Whitelam and R. L. Jack, "The statistical mechanics of dynamic pathways to self-assembly," Annu. Rev. Phys. Chem. **66**, 143 (2015).
[2]S. K. Kumar, G. Kumaraswamy, B. L. V. Prasad, R. Bandyopadhyaya, S. Granick, O. Gang, V. N. Manoharan, D. Frenkel, and N. A. Kotov, "Nanoparticle assembly: A perspective and some unanswered questions," Curr. Sci. **112**, 1635 (2017).
[3]N. C. Seeman and H. F. Sleiman, "DNA nanotechnology," Nat. Rev. Mater. **3**(1), 17068 (2017).
[4]W. Liu, M. Tagawa, H. L. Xin, T. Wang, H. Emamy, H. Li, K. G. Yager, F. W. Starr, A. V. Tkachenko, and O. Gang, "Diamond family of nanoparticle superlattices," Science **351**, 582 (2016).
[5]T. Zhang, C. Hartl, K. Frank, A. Heuer-Jungemann, S. Fischer, P. C. Nickels, B. Nickel, and T. Liedl, "3D DNA origami crystals," Adv. Mater. **30**, 1800273 (2018).
[6]D. Kashchiev, P. G. Vekilov, and A. B. Kolomeisky, "Kinetics of two-step nucleation of crystals," J. Chem. Phys. **122**, 244706 (2005).
[7]D. Erdemir, A. Y. Lee, and A. S. Myerson, "Nucleation of crystals from solution: Classical and two-step models," Acc. Chem. Res. **42**, 621 (2009).
[8]P. G. Vekilov, "The two-step mechanism of nucleation of crystals in solution," Nanoscale **2**, 2346 (2010).
[9]G. I. Tóth, T. Pusztai, G. Tegze, G. Tóth, and L. Gránásy, "Amorphous nucleation precursor in highly nonequilibrium fluids," Phys. Rev. Lett. **107**, 175702 (2011).
[10]R. P. Sear, "The non-classical nucleation of crystals: Microscopic mechanisms and applications to molecular crystals, ice and calcium carbonate," Int. Mater. Rev. **57**, 328 (2012).
[11]T. K. Haxton, L. O. Hedges, and S. Whitelam, "Crystallization and arrest mechanisms of model colloids," Soft Matter **11**, 9307 (2015).
[12]J. Russo and H. Tanaka, "Nonclassical pathways of crystallization in colloidal systems," MRS Bull. **41**, 369 (2016).
[13]G. C. Sosso, J. Chen, S. J. Cox, M. Fitzner, P. Pedevilla, A. Zen, and A. Michaelides, "Crystal nucleation in liquids: Open questions and future challenges in molecular dynamics simulations," Chem. Rev. **116**, 7078 (2016).
[14]J. F. Lutsko, "How crystals form: A theory of nucleation pathways," Sci. Adv. **5**, eaav7399 (2019).
[15]D. James, S. Beairsto, C. Hartt, O. Zavalov, I. Saika-Voivod, R. K. Bowles, and P. H. Poole, "Phase transitions in fluctuations and their role in two-step nucleation," J. Chem. Phys. **150**, 074501 (2019).
[16]C. Desgranges and J. Delhommelle, "Can ordered precursors promote the nucleation of solid solutions?," Phys. Rev. Lett. **123**, 195701 (2019).
[17]D. Kashchiev, "Classical nucleation theory approach to two-step nucleation of crystals," J. Cryst. Growth **530**, 125300 (2020).
[18]S. Lee, E. G. Teich, M. Engel, and S. C. Glotzer, "Entropic colloidal crystallization pathways via fluid–fluid transitions and multidimensional prenucleation motifs," Proc. Natl. Acad. Sci. U. S. A. **116**, 14843 (2019).
[19]P. R. t. Wolde and D. Frenkel, "Enhancement of protein crystal nucleation by critical density fluctuations," Science **277**, 1975 (1997).
[20]P. Tan, N. Xu, and L. Xu, "Visualizing kinetic pathways of homogeneous nucleation in colloidal crystallization," Nat. Phys. **10**, 73 (2014).
[21]H. Jiang, P. G. Debenedetti, and A. Z. Panagiotopoulos, "Nucleation in aqueous NaCl solutions shifts from 1-step to 2-step mechanism on crossing the spinodal," J. Chem. Phys. **150**, 124502 (2019).
[22]D. Gebauer, A. Völkel, and H. Cölfen, "Stable prenucleation calcium carbonate clusters," Science **322**, 1819 (2008).
[23]E. M. Pouget, P. H. H. Bomans, J. A. C. M. Goos, P. M. Frederik, G. de With, and N. A. J. M. Sommerdijk, "The initial stages of template-controlled $CaCO_3$ formation revealed by cryo-TEM," Science **323**, 1455 (2009).
[24]D. Fusco and P. Charbonneau, "Crystallization of asymmetric patchy models for globular proteins in solution," Phys. Rev. E **88**, 012721 (2013).
[25]S. James, M. K. Quinn, and J. J. McManus, "The self assembly of proteins; probing patchy protein interactions," Phys. Chem. Chem. Phys. **17**, 5413 (2015).
[26]J. J. McManus, P. Charbonneau, E. Zaccarelli, and N. Asherie, "The physics of protein self-assembly," Curr. Opin. Colloid Interface Sci. **22**, 73 (2016).
[27]D. Fusco and P. Charbonneau, "Soft matter perspective on protein crystal assembly," Colloids Surf., B **137**, 22 (2016).
[28]A.-Y. Jee, K. Lou, H.-S. Jang, K. H. Nagamanasa, and S. Granick, "Nanoparticle puzzles and research opportunities that go beyond state of the art," Faraday Discuss. **186**, 11 (2016).
[29]M. Dijkstra and E. Luijten, "From predictive modelling to machine learning and reverse engineering of colloidal self-assembly," Nat. Mater. **20**, 762 (2021).

[30]S. Whitelam and I. Tamblyn, "Learning to grow: Control of material self-assembly using evolutionary reinforcement learning," Phys. Rev. E **101**, 052604 (2020).
[31]A. Bupathy, D. Frenkel, and S. Sastry, "Temperature protocols to guide selective self-assembly of competing structures," Proc. Natl. Acad. Sci. U. S. A. **119**, e2119315119 (2022).
[32]S. Whitelam and I. Tamblyn, "Neuroevolutionary learning of particles and protocols for self-assembly," Phys. Rev. Lett. **127**, 018003 (2021).
[33]M. C. Rechtsman, F. H. Stillinger, and S. Torquato, "Optimized interactions for targeted self-assembly: Application to a honeycomb lattice," Phys. Rev. Lett. **95**, 228301 (2005).
[34]É. Marcotte, F. H. Stillinger, and S. Torquato, "Optimized monotonic convex pair potentials stabilize low-coordinated crystals," Soft Matter **7**, 2332 (2011).
[35]É. Marcotte, F. H. Stillinger, and S. Torquato, "Communication: Designed diamond ground state via optimized isotropic monotonic pair potentials," J. Chem. Phys. **138**, 061101 (2013).
[36]G. Zhang, F. Stillinger, and S. Torquato, "Probing the limitations of isotropic pair potentials to produce ground-state structural extremes via inverse statistical mechanics," Phys. Rev. E **88**, 042309 (2013).
[37]M. Z. Miskin, G. Khaira, J. J. de Pablo, and H. M. Jaeger, "Turning statistical physics models into materials design engines," Proc. Natl. Acad. Sci. U. S. A. **113**, 34 (2016).
[38]B. A. Lindquist, R. B. Jadrich, and T. M. Truskett, "Communication: Inverse design for self-assembly via on-the-fly optimization," J. Chem. Phys. **145**, 111101 (2016).
[39]D. Chen, G. Zhang, and S. Torquato, "Inverse design of colloidal crystals via optimized patchy interactions," J. Phys. Chem. B **122**, 8462 (2018).
[40]R. Kumar, G. M. Coli, M. Dijkstra, and S. Sastry, "Inverse design of charged colloidal particle interactions for self assembly into specified crystal structures," J. Chem. Phys. **151**, 084109 (2019).
[41]É. Ducrot, M. He, G.-R. Yi, and D. J. Pine, "Colloidal alloys with preassembled clusters and spheres," Nat. Mater. **16**, 652 (2017).
[42]D. R. Nelson, "Toward a tetravalent chemistry of colloids," Nano Lett. **2**, 1125 (2002).
[43]V. N. Manoharan, M. T. Elsesser, and D. J. Pine, "Dense packing and symmetry in small clusters of microspheres," Science **301**, 483 (2003).
[44]Z. Zhang, A. S. Keys, T. Chen, and S. C. Glotzer, "Self-assembly of patchy particles into diamond structures through molecular mimicry," Langmuir **21**, 11547 (2005).
[45]F. Romano, J. Russo, and H. Tanaka, "Influence of patch-size variability on the crystallization of tetrahedral patchy particles," Phys. Rev. Lett. **113**, 138303 (2014).
[46]J. D. Halverson and A. V. Tkachenko, "DNA-programmed mesoscopic architecture," Phys. Rev. E **87**, 062310 (2013).
[47]F. Romano and F. Sciortino, "Patterning symmetry in the rational design of colloidal crystals," Nat. Commun. **3**, 975 (2012).
[48]D. F. Tracey, E. G. Noya, and J. P. K. Doye, "Programming patchy particles to form complex periodic structures," J. Chem. Phys. **151**, 224506 (2019).
[49]F. Romano, J. Russo, L. Kroc, and P. Šulc, "Designing patchy interactions to self-assemble arbitrary structures," Phys. Rev. Lett. **125**, 118003 (2020).
[50]J. Russo, F. Romano, L. Kroc, F. Sciortino, L. Rovigatti, and P. Šulc, "SAT-assembly: A new approach for designing self-assembling systems," J. Phys.: Condens. Matter **34**, 354002 (2022).
[51]L. Rovigatti, J. Russo, F. Romano, M. Matthies, L. Kroc, and P. Šulc, "A simple solution to the problem of self-assembling cubic diamond crystals," Nanoscale **14**, 14268 (2022).
[52]C. Desgranges and J. Delhommelle, "Unraveling the coupling between demixing and crystallization in mixtures," J. Am. Chem. Soc. **136**, 8145 (2014).
[53]Y. Wang, A. Lomakin, J. J. McManus, O. Ogun, and G. B. Benedek, "Phase behavior of mixtures of human lens proteins gamma D and beta B1," Proc. Natl. Acad. Sci. U. S. A. **107**, 13282 (2010).
[54]Y. Wang, A. Lomakin, R. F. Latypov, and G. B. Benedek, "Phase separation in solutions of monoclonal antibodies and the effect of human serum albumin," Proc. Natl. Acad. Sci. U. S. A. **108**, 16606 (2011).
[55]M. Heidenreich, J. M. Georgeson, E. Locatelli, L. Rovigatti, S. K. Nandi, A. Steinberg, Y. Nadav, E. Shimoni, S. A. Safran, J. P. K. Doye, and E. D. Levy, "Designer protein assemblies with tunable phase diagrams in living cells," Nat. Chem. Biol. **16**, 939 (2020).
[56]G. van Anders, N. K. Ahmed, R. Smith, M. Engel, and S. C. Glotzer, "Entropically patchy particles: Engineering valence through shape entropy," ACS Nano **8**, 931 (2013).
[57]Z. Zhang and S. C. Glotzer, "Self-assembly of patchy particles," Nano Lett. **4**, 1407 (2004).
[58]A. B. Pawar and I. Kretzschmar, "Fabrication, assembly, and application of patchy particles," Macromol. Rapid Commun. **31**, 150 (2010).
[59]E. Bianchi, R. Blaak, and C. N. Likos, "Patchy colloids: State of the art and perspectives," Phys. Chem. Chem. Phys. **13**, 6397 (2011).
[60]F. Romano and F. Sciortino, "Colloidal self-assembly: Patchy from the bottom up," Nat. Mater. **10**, 171 (2011).
[61]K. Suzuki, K. Hosokawa, and M. Maeda, "Controlling the number and positions of oligonucleotides on gold nanoparticle surfaces," J. Am. Chem. Soc. **131**, 7518 (2009).
[62]J.-W. Kim, J.-H. Kim, and R. Deaton, "DNA-linked nanoparticle building blocks for programmable matter," Angew. Chem., Int. Ed. **50**, 9185 (2011).
[63]Y. Wang, Y. Wang, D. R. Breed, V. N. Manoharan, L. Feng, A. D. Hollingsworth, M. Weck, and D. J. Pine, "Colloids with valence and specific directional bonding," Nature **491**, 51 (2012).
[64]L. Feng, R. Dreyfus, R. Sha, N. C. Seeman, and P. M. Chaikin, "DNA patchy particles," Adv. Mater. **25**, 2779 (2013).
[65]P. W. K. Rothemund, "Folding DNA to create nanoscale shapes and patterns," Nature **440**, 297 (2006).
[66]Y. Tian, J. R. Lhermitte, L. Bai, T. Vo, H. L. Xin, H. Li, R. Li, M. Fukuto, K. G. Yager, J. S. Kahn *et al.*, "Ordered three-dimensional nanomaterials using DNA-prescribed and valence-controlled material voxels," Nat. Mater. **19**, 789 (2020).
[67]W. Bol, "Monte Carlo simulations of fluid systems of waterlike molecules," Mol. Phys. **45**, 605 (1982).
[68]N. Kern and D. Frenkel, "Fluid–fluid coexistence in colloidal systems with short-ranged strongly directional attraction," J. Chem. Phys. **118**, 9882 (2003).
[69]L. Rovigatti, J. Russo, and F. Romano, "How to simulate patchy particles," Eur. Phys. J. E **41**, 59 (2018).
[70]C. Beneduce, F. Sciortino, P. Sulc, and J. Russo, "How to include azeotropy in the design of self-assembling patchy particles systems," arXiv:2208.09856 (2022).
[71]M. Rubinstein, R. H. Colby *et al.*, *Polymer Physics* (Oxford University Press, New York, 2003), Vol. 23.
[72]H. Tanaka, H. Tong, R. Shi, and J. Russo, "Revealing key structural features hidden in liquids and glasses," Nat. Rev. Phys. **1**, 333 (2019).
[73]W. Lechner and C. Dellago, "Accurate determination of crystal structures based on averaged local bond order parameters," J. Chem. Phys. **129**, 114707 (2008).
[74]D. Frenkel and B. Smit, *Understanding Molecular Simulation: From Algorithms to Applications* (Elsevier, 2001), Vol. 1.
[75]L. Xu, S. V. Buldyrev, H. E. Stanley, and G. Franzese, "Homogeneous crystal nucleation near a metastable fluid-fluid phase transition," Phys. Rev. Lett. **109**, 095702 (2012).
[76]A. Stukowski, "Visualization and analysis of atomistic simulation data with OVITO–the Open Visualization Tool," Modell. Simul. Mater. Sci. Eng. **18**, 015012 (2010).
[77]I. Chakraborty, D. J. G. Pearce, R. W. Verweij, S. C. Matysik, L. Giomi, and D. J. Kraft, "Self-assembly dynamics of reconfigurable colloidal molecules," ACS Nano **16**, 2471 (2022).
[78]Y. Xiong, S. Yang, Y. Tian, A. Michelson, S. Xiang, H. Xin, and O. Gang, "Three-dimensional patterning of nanoparticles by molecular stamping," ACS Nano **14**, 6823 (2020).
[79]J. Russo, F. Leoni, F. Martelli, and F. Sciortino, "The physics of empty liquids: From patchy particles to water," Rep. Prog. Phys. **85**, 016601 (2021).

[80]E. Bianchi, J. Largo, P. Tartaglia, E. Zaccarelli, and F. Sciortino, "Phase diagram of patchy colloids: Towards empty liquids," Phys. Rev. Lett. **97**, 168301 (2006).
[81]F. Romano, E. Sanz, and F. Sciortino, "Crystallization of tetrahedral patchy particles in silico," J. Chem. Phys. **134**, 174502 (2011).
[82]I. Altan and P. Charbonneau, "Obtaining soft matter models of proteins and their phase behavior," in *Protein Self-Assembly* (Springer, 2019), pp. 209–228.
[83]N. Gnan, F. Sciortino, and E. Zaccarelli, "Patchy particle models to understand protein phase behavior," in *Protein Self-Assembly* (Springer, 2019), pp. 187–208.
[84]J. J. McManus, *Protein Self-Assembly* (Springer, 2019).
[85]T. V. Hvozd, Y. V. Kalyuzhnyi, V. Vlachy, and P. T. Cummings, "Empty liquid state and re-entrant phase behavior of the patchy colloids confined in porous media," J. Chem. Phys. **156**, 161102 (2022).